Mid-infrared free-space cryptosystem

Olivier Spitz, Andreas Herdt, Pierre Didier, Wolfgang Elsäßer, Frédéric Grillot

NOLTA, IEICE

Paper

Mid-infrared free-space cryptosystem

Olivier Spitz [1 a)], *Andreas Herdt* [2], *Pierre Didier* [1], *Wolfgang Elsäßer* [2], *and Frédéric Grillot* [1,3]

[1] *LTCI, Télécom Paris, Institut Polytechnique de Paris*
19 place Marguerite Perey, 91120 Palaiseau, France

[2] *Institut für Angewandte Physik, Technische Universität Darmstdat*
Schloßgartenstraße 7, D-64289 Darmstadt, Germany

[3] *Centre for High Technology Materials, University of New-Mexico*
1313 Goddard SE, Albuquerque, NM 87106, USA

[a)] *olivier.spitz@telecom-paris.fr*

Received July 10, 2021; Revised August 30, 2021; Published January 1, 2022

Abstract: Communication privacy is one of the key requirements for always expanding networks. Furthermore, fibre systems are becoming saturated and many remote areas do not have access to broadband connection because current systems are too difficult or expensive to deploy. In this work, we experimentally demonstrate a mid-infrared free-space cryptosystem that is based on chaos synchronization between two quantum cascade lasers. Optimal amplitude conditions to ensure both privacy and acceptable deciphering are described, paving the way towards a wide adoption of quantum cascade lasers for future communication systems.

Key Words: quantum cascade laser, free-space optics, private communication, non-linear dynamics, semiconductor laser, mid-infrared photonics

1. Introduction

The quantum cascade laser (QCL) technology has known tremendous improvements in the past two decades, boosted by the need for mid-infrared frequency combs for precision spectroscopy [1] and high-power low-divergence beams [2] for military applications. There is nowadays a growing interest for high-speed devices relying on quantum well and quantum cascade structures either on the emission side [3] or on the reception side [4, 5], even if QCLs for free-space communication has long been envisioned [6]. The main advantage of mid-infrared wavelength is that it is less affected by atmospheric conditions than near-infrared wavelength, thus the superiority of mid-infrared light for long-range free-space transmission [7]. On top of that, the directivity of the beam, as well as the stealth conferred by the background emission, makes communication systems based on QCLs very desirable [8]. Directive emission is however not sufficient to ensure the privacy of a free-space communication and subsequent encoding, either in the message itself or at the physical layer, is required. A lot of attention has been directed towards quantum key distribution (QKD) as it can offer maximum level of privacy because the secret keys used to encrypt and decrypt messages are encoded using properties of quantum physics [9]. The most advanced achievements in terms of QKD are in the range of a few bits per second even though long-distance transmission can now be envisioned [10]. In addition, the implementation of

Nonlinear Theory and Its Applications, IEICE, vol. 13, no. 1, pp. 44–52 DOI: 10.1587/nolta.13.44

QKD is still very complex and hinders the large-scale deployment of such powerful tool [11]. In order to overcome the low data rate and the absence of QKD technology in the mid-infrared, new methods are developed in that optical domain, such as compound laser states [12] using mutually coupled interband cascade lasers (ICLs). Another technique relies on chaos synchronization and has been experimentally investigated in semiconductor lasers since 1999 [13], then extended to several fibred configurations [14, 15]. This method is easy to implement and allows high-speed private fibred communication up to dozens of Gbits/s and hundreds of kilometers [16]. This feat is made possible because of the large chaos bandwidth exhibited by many semiconductor lasers [17], such as laser diodes and VCSELs. QCLs are intersubband semiconductor lasers and consequently, they do not exhibit relaxation oscillations [18]. This property theoretically means a strong potential for very high-speed non-linear dynamics, up to hundreds of GHz [19], because such bandwidth is generally bounded by the relaxation frequency [20]. However, QCLs exhibit a complex material structure and, up to date, their maximum chaos bandwidth under external optical feedback is limited to a few dozens of MHz [21]. On the one hand, this could be a limitation to their use in private communication systems but, on the other hand, their potential for hyperchaos (i.e. chaos dynamics with at least two positive Lyapunov exponents [22]), their high optical power and their wavelength of operation are in favor of a wide use for this now mature technology. The experimental effort we present focuses on a free-space mid-infrared cryptosystem and on the chaos synchronization parameters. This work shows that a compromise must be found between a transmission that is immune to eavesdroppers' attack and an easy recovery for the legitimate user. Overall, this study is of utter interest for the development of private communication system in the mid-infrared, with a view towards implementation in a real-field environment.

2. Methods

In this experiment, we use two distributed-feedback (DFB) QCLs emitting at 5.7 μm and with parameters which are matched to the best extent, because this is one of the conditions to optimize message extraction after chaos synchronization [23]. For both lasers, the waveguide is 2 mm-long and 14 μm-wide and the QCLs emit CW at room temeprature. Figure 1 depicts the experimental setup for the mid-infrared free-space cryptosystem. In the transmitter box, the first QCL (that is called the master), is driven chaotic with the external optical feedback caused by the mirror. Rotating the polarizer in front of the feedback mirror allows selecting the most appropriate hyperchaos for private communication. The 60 % reflection coefficient of the beam splitter is ideal to achieve high feedback ratio that is often required to trigger complex non-linear dynamics in QCLs [24]. It is relevant to note that the return-to-zero (RZ) message to be transmitted [25] is loaded to an arbitrary waveform generator (AWG) and then injected at the level of the current source with a 0.4 A/V ratio. This means that the message is already included in the beam hitting the feedback mirror and that conforms the chaos waveform. This waveform is then optically injected into another QCL (that is called the slave),

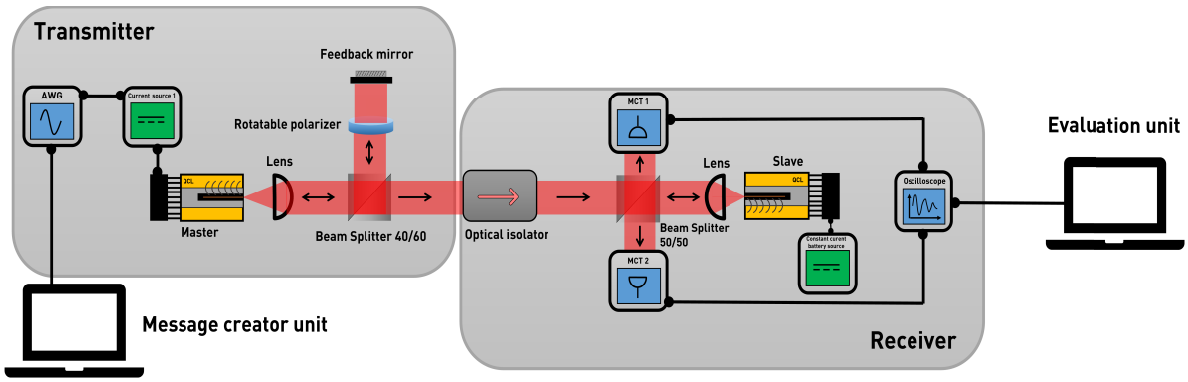

Fig. 1. Experimental setup for private free-space communication based on chaos synchronization. The chaotic master QCL is an external-cavity laser and the slave QCL is free-running before optical injection. AWG: arbitrary waveform generator; MCT: Mercury-Cadmium Telluride detector.

placed at roughly one meter from the master in the receiver box.

Before the optical injection process, the slave QCL is not chaotic because it is not in an external-cavity configuration. The light from the slave is quenched by an optical isolator on its way to the master laser because we do not want to study a mutual injection scheme. The optical wavelength of the two lasers is precisely matched by tuning the temperature and the bias current, even if we will see in the following that the master laser can excite one of the slave suppressed side-modes without detrimental degradation of the chaos synchronization. To maximize the optical power of both QCLs, the master is housed in a LDM-4872 mount and cooled down to -22°C while the slave is housed in a LDM-4872 mount and cooled down to 5°C. The optical signal of the master QCL, with the embedded private message, is received by the first Mercury-Cadmium-Telluride detector (MCT1) while the optical signal of the slave QCL is received by MCT2. The bandwidth of these two detectors is of several hundreds of MHz and this does not limit the private transmission rate. In the following, we will focus on a data rate of 0.5 Mbits/s because the QCL chaos bandwidth is approximately 5 MHz and the message electrical spectrum must be included in the chaos electrical bandwidth [26]. Once retrieved by the oscilloscope, the master timetrace and the slave timetrace are recorded and time-shifted to account for the time of flight between the transmitter and the receiver. The timetraces are then filtered as the message sequence to be deciphered has a limited bandwidth. This step allows removing the high-frequency noise [27] that is clearly seen in the slave signal, as we will see hereafter. After filtering, a subtraction process between the master and the slave timetrace produces a new timetrace that we will call difference in the following. If the deciphering process is optimized, this difference timetrace is a copy of the initial message that was concealed within the master optical chaos.

3. Results

3.1 Implementation of the private message at the master level

In the following, we highlight the experimental results for various amplitudes of the initial message that is hidden by the master chaos. Figure 2 shows the whole chaos private communication process for a 3 mV message, which is equivalent to a maximum bias amplitude of 1.2 mA that is injected to the master QCL. As the master QCL is continusously biased at 700 mA, this represents a small amplitude elctrical modulation. Figure 2 (a) shows the unfiltered master signal in red and the unfil-

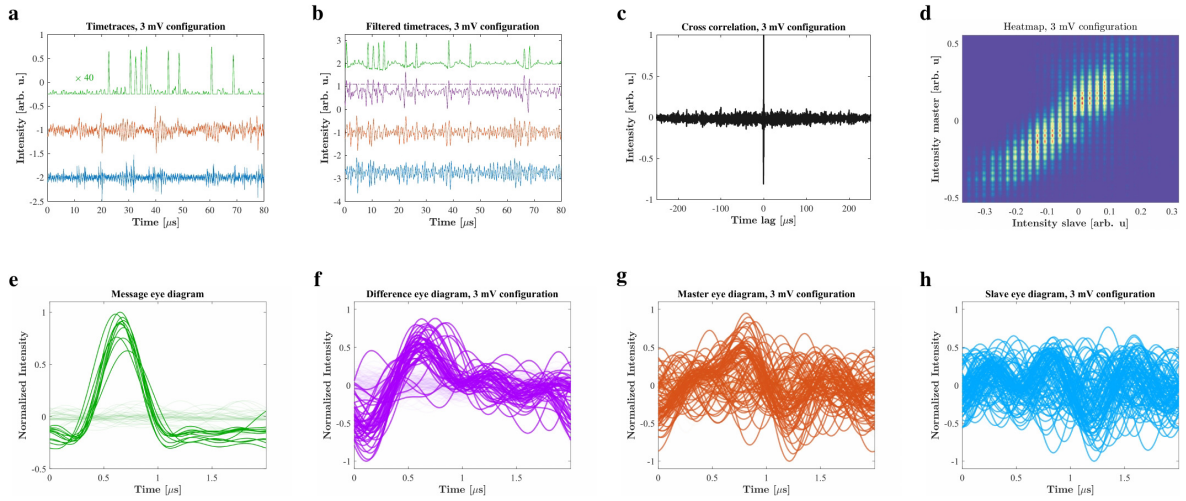

Fig. 2. Private communication with a 3 mV message; the initial message corresponds to the green traces, the master signal corresponds to the red traces, the slave signal corresponds to the blue traces, the difference signal corresponds to the purple traces. (a) unfiltered timetraces; (b) filtered timetraces, the dash-dotted line sets the limit between the 0 bits and the 1 bits during the analysis of the purple trace; (c) time correlation between the master and the slave timetrace; (d) intensity correlation between the master and the slave timetrace; (e - f) eye diagrams to assess the quality of the transmission.

tered slave signal in blue, as well as the initial message in green that is concealed and that is strongly magnified to be comparable with the chaos timetraces. As our MCTs are high-pass detectors, all the waveforms amplitude should be centered around zero but they are vertically shifted for clarity. Chaos synchronization between the red and the blue signal is clear but the blue signal is sometimes degraded by high-frequency noise. This noise could be explained by the small optical wavelength detuning between the master and the slave. This phenomenon has aleady been observed in free-running injected QCLs and is very sensitive to the bias current [28] and hence varying with time in our configuration. Figure 2 (b) shows the recovery process with the previous timetraces that have been filtered and the difference timetrace in purple. One can see in this panel that the difference timetrace is not a perfect copy of the initial message and, if we take into account the whole recorded timetrace (not shown here), the error rate is 3.7 %. One of the levers to avoid error in the deciphering process would be to increase the amplitude of the injected message and this will be discussed in the next paragraph. Apart from the error rate during the recovery process, one has to focus on the privacy of the message when it is hidden among the optical chaos and an eavesdropper attempts to extract it. Figure 2 (c) shows that high correlation only occurs for a single time lag corresponding to the time of flight between the master and the slave. This means that, even if the message sequence to be transmitted is repeated every 100 μs, there is no dependence on any previous chaotic outcome, and this is expected for private operation. The quality of the synchronization between the master and the slave is assessed in Fig. 2 (d). For two perfectly synchronized QCLs, the correlation heatmap would be a straight line with a positive gradient but in experimental conditions, the diagram always shows scattering caused by imperfections. Finally, four eye diagrams (EDs) can be visualized in Fig. 2 (e - h). The eye diagram is the superposition of all the bits on the same time interval, which is 2 μs in our case because the data rate is 0.5 Mbits/s, and is a convenient representation of the quality of deciphering. For each ED, bits deciphered as 0 are drawn with a light color while bits deciphered as 1 are drawn with a stressed color. The initial message ED is shown in Fig. 2 (e) and one clearly observes the shape of a RZ pattern. For the difference signal ED (Fig. 2 (f)), the shape of the initial pattern can be partially seen and this is in accordance with the recovery process that is not error-free. What is more relevant for our analysis is the shape of the ED for the master signal and the slave signal, Fig. 2 (g) and (h), respectively. Though the master signal is filtered with the most appropriate filter (which is theoretically not accessible for the eavesdropper), it is very difficult to extract the shape of the initial bit pattern in Fig. 2 (g) and this is also confirmed by the red trace in Fig. 2 (b) where no sign of the 1 bits can be spotted. If we take into account the whole recorded timetrace (not shown here), the error rate for an eavesdropper with the matching filter is 23%. This value can be compared with the lower limit commonly accepted for a non-decipherable transmission, which is an error rate of 25% [29]. Note that in our case, we have supposed that the eavesdropper has access to the best-matching filter, and this strongly helps in deciphering the encoded message. Yet, the error rate remains close to 25%.

Figure 3 corresponds to the same analysis but for a 4 mV message, which is equivalent to a maximum bias amplitude of 1.6 mA. Figure 3 (a) shows the unfiltered chaos synchronization with no discernable difference compared to the previous case. After filtering and subtraction, the message is now clearly visible in the difference timetrace, with also the advent of a strong undershoot before each 1 bit. This is illustrated in Fig. 3 (b). The cross correlation diagram in Fig. 3 (c) still shows a predominant correlation but there are also some side-modes at $\pm$ 100 and $\pm$ 200 μs, and this indicates that there is a minor correlation between consecutive sequences. Looking at the details in the red and blue timetraces in Fig. 3 (b) as well as looking at the correlation heatmap in Fig. 3 (d), one can conclude that the synchronization has improved. Figure 3 (f) shows the ED for the difference timetrace, which corresponds to an error-free private communication. One can again notice the strong undershoot occuring before the 1 bits and further inquiry is required to explain such distortion in the difference timetrace. Even if the bit pattern is definitely clearer in the ED of difference than in the ED of master (Fig. 3 (g)), the red trace shows a larger distorted pulse and, with this 4 mV message amplitude, the eavesdropper's error rate is only 5.2 % and the privacy of the transmission is threatened. Yet, one has to keep in mind that this ED is obtained with matching filter and it is very unlikely that the eavesdropper has access to that filter.

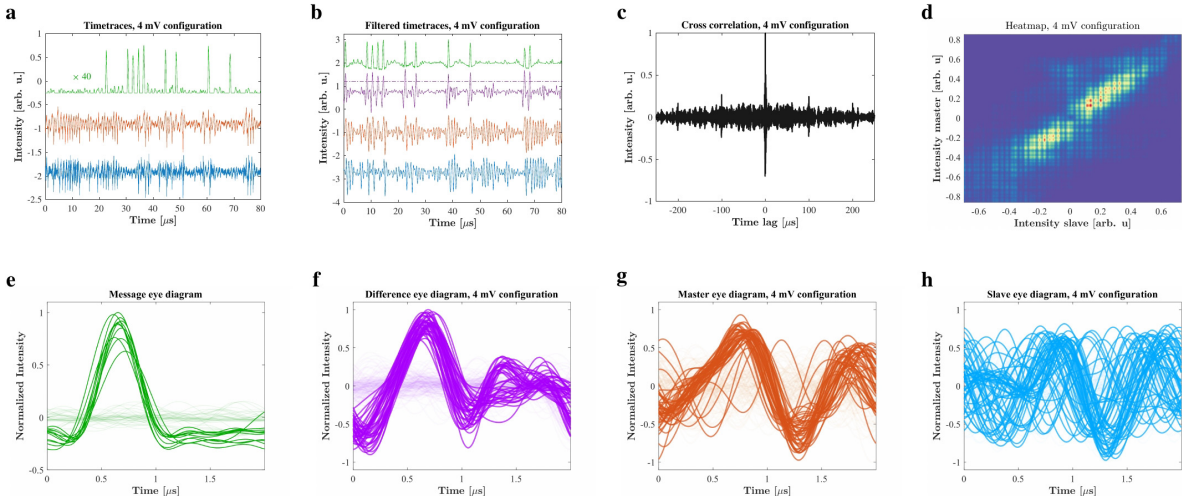

Fig. 3. Private communication with a 4 mV message; the initial message corresponds to the green traces, the master signal corresponds to the red traces, the slave signal corresponds to the blue traces, the difference signal corresponds to the purple traces. (a) unfiltered timetraces; (b) filtered timetraces, the dash-dotted line sets the limit between the 0 bits and the 1 bits during the analysis of the purple trace; (c) time correlation between the master and the slave timetrace; (d) intensity correlation between the master and the slave timetrace; (e - f) eye diagrams to assess the quality of the transmission.

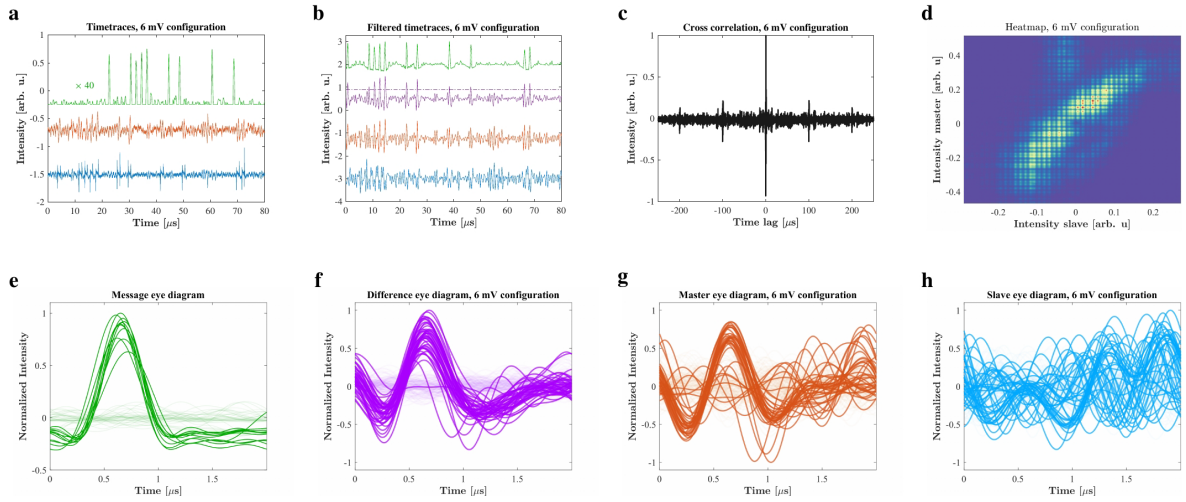

Fig. 4. Private communication with a 6 mV message; the initial message corresponds to the green traces, the master signal corresponds to the red traces, the slave signal corresponds to the blue traces, the difference signal corresponds to the purple traces. (a) unfiltered timetraces; (b) filtered timetraces, the dash-dotted line sets the limit between the 0 bits and the 1 bits during the analysis of the purple trace; (c) time correlation between the master and the slave timetrace; (d) intensity correlation between the master and the slave timetrace; (e - f) eye diagrams to assess the quality of the transmission.

The configuration with a 6 mV message is depicted in Fig. 4. The message is no longer well concealed in the chaos timetrace, even without matching filter, as shown in Fig. 4 (a) for the red trace. This is even more noticeable in Fig. 4 (b), after filtering. The difference timetrace still allows recovering the message but the privacy is detrimentally degraded. Even if the message amplitude in Fig. 4 is only twice the message amplitude in Fig. 2, the optical feedback process seems to magnify the pulse response. This could be linked to the extreme event phenomenon in QCLs [30], where electrical bursts with specific properties are strongly enhanced in a non-linear process. The correlation between consecutive sequences is also increased, as underlined by the spikes at $\pm$ 100 and $\pm$ 200 μs in Fig. 4 (c) and, contrary to the previous case, the amplitude increase leads to a degradation of the synchronization

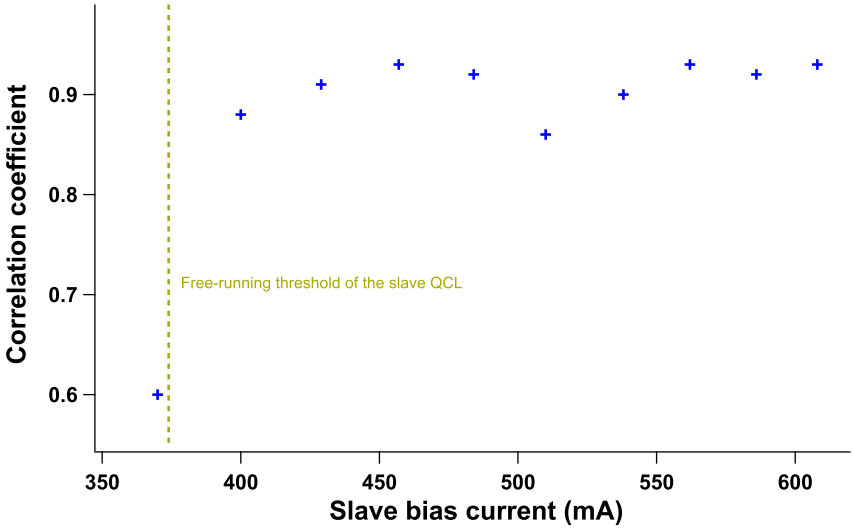

Fig. 5. Quality of the chaos synchronization when the master bias is fixed at 750 mA and the slave bias is varied. All the synchronization currents are shown with blue crosses. Outside of these markers, synchronization does not occur and the correlation coefficient is in the order of 0.1.

that is visualized in the correlation heatmap of Fig. 4 (d). Figures 4 (f) and (g) show two similar EDs, the exact shape of the bit is now recovered by the eavesdropper only with the matching filter. Because we use basic threshold detection to discriminate 0 and 1 bits, the eavesdropper's error rate is now 11.5 %, which is a larger value compared to the previous 4 mV case. However, the 6 mV configuration gives a more realistic image of the bit pattern for a potential eavesdropper, which could help extracting the concealed message and this further jeopardizes the privacy of the transmission.

3.2 Bias current of the slave laser

When performing chaos synchronization, two sets of frequencies must be matched so that the synchronization is effective. The first one is the electrical frequency component and that corresponds to the non-linear pattern presented in the previous figures. In other words, the slave laser reproduces the chaos timetrace generated by the master laser. However, this is only possible if the second frequency parameter is also matched. This occurs when the optical wavelength of the slave and that of the master are the same [31]. This wavelength corresponds to a very high frequency when compared to the non-linear dynamics. Because we are working with mono-mode QCLs, it is possible to determine the optical wavelength and to tune the temperature or bias current of one of the lasers (generally the slave) to perform the matching. Yet, the DFB QCLs have suppressed side-modes and it is possible to excite one of the side-modes of the slave when the master emits precisely at this wavelength [32]. The activation of such modes means that it is possible to perform chaos synchronization for various current detunings between the master and the slave. Figure 5 shows the quality of the synchronization when varying the bias current of the slave laser whereas the bias current of the master laser is kept constant at 750 mA. When the Pearson correlation coeffcient is close to 1, the slave is well synchonized with the master [33]. One can see that the synchronization is effective in our case when the slave laser is biased above threshold and when the bias current is varied by 26 $\pm$ 4 mA from 400 mA to 608 mA. This current step induces a local temperature change even if the LDM-4872 mount is kept at constant temperature, and the optical wavelength of the slave is changed, which means that the suppressed side-modes also shift and can be excited. As the suppressed side-modes are equally spaced, it is not surprising that one can excite them by varying the slave bias current with an almost constant step. For each current value shown in Fig. 5, the synchronization can be observed around this value but for a current shift below $\pm$ 0.5 mA. For other current values, the chaos synchronization is lost because the frequency-pulling effect [34] from the master QCL is not strong enough to excite one of the modes of the slave QCL. Intriguingly, the slave can be chaos synchronized just below the free-running threshold even if the correlation coefficient is 0.6 in that case, while it is between 0.86

and 0.93 above threshold. Below threshold, DFB QCLs are multi-mode [35] but the injected light from the master can be enough to favor a mono-mode operation, provided that the slave is just below the free-running threshold. At 0.6, the synchronization is still effective because when the bias of the slave QCL is different from the values shown in Fig. 5, the typical correlation coefficient is 0.1.

4. Conclusions

This work describes a mid-infrared free-space cryptosystem and analyzes the deciphering conditions when the signals are well filtered, from the viewpoint of a legitimate user and from the viewpoint of an illegitimate user. We have shown that a large amplitude message degrades the privacy of the transmission. This is in good agreement with the litterature and one has to ensure that a 1 bit induces not more than a 10 % increase of the average laser intensity [31]. This trade-off leads to a small-amplitude message enciphering and complicates the deciphering process for the legitimate user, who will further need error-correction code to retrieve the correct bit sequence. We have also demonstrated that synchronization can occur for several bias currents at the slave level when the master bias is fixed and this is explained by the frequency-pulling effect on the slave's suppressed side-modes when the master is uni-directionally injected into the slave. For the various synchronization conditions above threshold, this does not degrade the quality of the correlation. Further studies will focus on chaos synchronization tentative with Fabry-Perot QCLs in order to understand the role of multi-mode injection, and on the development of versatile end-user applications.

Acknowledgments

This work is supported by the French Defense Agency (DGA), the French ANR program (ANR-17-ASMA-0006), the European Office of Aerospace Research and Development (FA9550-18-1-7001). Authors thank Dr. Mathieu Carras from mirSense for providing quantum cascade lasers and thank Dr. Chadi Jabbour for lending some of the equipment used in this work.

References

[1] A. Schliesser, N. Picqué, and T.W. Hänsch, "Mid-infrared frequency combs," *Nature Photonics*, vol. 6, no. 7, pp. 440–449, 2012.

[2] D. Botez, J.D. Kirch, C. Boyle, K.M. Oresick, C. Sigler, H. Kim, B.B. Knipfer, J.H. Ryu, D. Lindberg, T. Earles, L.J. Mawst, and Y.V. Flores, "High-efficiency, high-power mid-infrared quantum cascade lasers," *Optical Materials Express*, vol. 8, no. 5, pp. 1378–1398, 2018.

[3] Y. Zhou, J. Liu, S. Zhai, N. Zhuo, J. Zhang, S. Liu, L. Wang, F. Liu, and Z. Wang, "High-speed operation of single-mode tunable quantum cascade laser based on ultra-short resonant cavity," *AIP Advances*, vol. 11, no. 1, p. 015325, 2021.

[4] J. Hillbrand, L.M. Krüger, S. Dal Cin, H. Knötig, J. Heidrich, A.M. Andrews, G. Strasser, U. Keller, and B. Schwarz, "High-speed quantum cascade detector characterized with a mid-infrared femtosecond oscillator," *Optics Express*, vol. 29, no. 4, pp. 5774–5781, 2021.

[5] M. Hakl, Q. Lin, S. Lepillet, M. Billet, J.F. Lampin, S. Pirotta, R. Colombelli, W. Wan, J.C. Cao, H. Li, E. Peytavit, and S. Barbieri, "Ultrafast Quantum-Well Photodetectors Operating at 10 μm with a Flat Frequency Response up to 70 GHz at Room Temperature," *ACS Photonics*, vol. 8, no. 2, pp. 464–471, 2021.

[6] S. Blaser, D. Hofstetter, M. Beck, and J. Faist, "Free-space optical data link using Peltier-cooled quantum cascade laser," *Electronics Letters*, vol. 37, no. 12, pp. 778–780, 2001.

[7] P. Corrigan, R. Martini, E.A. Whittaker, and C. Bethea, "Quantum cascade lasers and the Kruse model in free space optical communication," *Optics Express*, vol. 17, no. 6, pp. 4355–4359, 2009.

[8] X. Pang, O. Ozolins, L. Zhang, R. Schatz, A. Udalcovs, X. Yu, G. Jacobsen, S. Popov, J. Chen, and S. Lourdudoss, "Free-space communications enabled by quantum cascade lasers," *physica status solidi (a)*, vol. 218, no. 3, p. 2000407, 2021.

[9] W. Li, V. Zapatero, H. Tan, K. Wei, H. Min, W.Y. Liu, X. Jiang, S.K. Liao, C.Z. Peng, M. Curty, F. Xu, and J.W. Pan, "Experimental quantum key distribution secure against malicious devices," *Physical Review Applied*, vol. 15, no. 3, p. 034081, 2021.

[10] H. Liu, C. Jiang, H.T. Zhu, M. Zou, Z.W. Yu, X.L. Hu, H. Xu, S. Ma, Z. Han, J.P. Chen, Y. Dai, S.B. Tang, W. Zhang, H. Li, L. You, Z. Wang, Y. Hua, H. Hu, H. Zhang, F. Zhou, Q. Zhang, X.B. Wang, T.Y. Chen, and J.W. Pan, "Field test of twin-field quantum key distribution through sending-or-not-sending over 428 km," *Physical Review Letters*, vol. 126, no. 25, p. 250502, 2021.

[11] E. Diamanti, H.K. Lo, B. Qi, and Z. Yuan, "Practical challenges in quantum key distribution," *npj Quantum Information*, vol. 2, no. 1, pp. 1–12, 2016.

[12] A. Herdt, *The laser-as-detector approach exploiting mid-infrared emitting interband cascade lasers: A potential for spectroscopy and communication applications*, Ph.D. dissertation, Technische Universität Darmstadt, 2020.

[13] S. Sivaprakasam and K.A. Shore, "Demonstration of optical synchronization of chaotic external-cavity laser diodes," *Optics letters*, vol. 24, no. 7, pp. 466–468, 1999.

[14] T. Heil, J. Mulet, I. Fischer, C.R. Mirasso, M. Peil, P. Colet, and W. Elsässer, "ON/OFF phase shift keying for chaos-encrypted communication using external-cavity semiconductor lasers," *IEEE Journal of Quantum Electronics*, vol. 38, no. 9, pp. 1162–1170, 2002.

[15] V. Annovazzi-Lodi, M. Benedetti, S. Merlo, M. Norgia, and B. Provinzano, "Optical chaos masking of video signals," *IEEE Photonics Technology Letters*, vol. 17, no. 9, pp. 1995–1997, 2005.

[16] J. Ke, L. Yi, G. Xia, and W. Hu, "Chaotic optical communications over 100-km fiber transmission at 30-Gb/s bit rate," *Optics Letters*, vol. 43, no. 6, pp. 1323–1326, 2018.

[17] K. Schires, S. Gomez, A. Gallet, G.H. Duan, and F. Grillot, "Passive chaos bandwidth enhancement under dual-optical feedback with Hybrid III–V/Si DFB laser," *IEEE Journal of Selected Topics in Quantum Electronics*, vol. 23, no. 6, pp. 1–9, 2017.

[18] R. Paiella, R. Martini, F. Capasso, C. Gmachl, H.Y. Hwang, D.L. Sivco, J.N. Baillargeon, A.Y. Cho, E.A. Whittaker, and H.C. Liu, "High-frequency modulation without the relaxation oscillation resonance in quantum cascade lasers," *Applied Physics Letters*, vol. 79, no. 16, pp. 2526–2528, 2001.

[19] N.N. Vukovic, J.V. Radovanovic, V.B. Milanovic, A.V. Antonov, D.I. Kuritsyn, V.V. Vaks, and D.L. Boiko, "Regular self-pulsations in external cavity mid-IR quantum cascade lasers," arXiv preprint arXiv:1902.00205, 2019.

[20] J. Mørk, J. Mark, and B. Tromborg, "Route to chaos and competition between relaxation oscillations for a semiconductor laser with optical feedback," *Physical Review Letters*, vol. 65, no. 16, p. 1999, 1990.

[21] L. Jumpertz, K. Schires, M. Carras, M. Sciamanna, and F. Grillot, "Chaotic light at mid-infrared wavelength," *Light: Science & Applications*, vol. 5, no. 6, p. e16088, 2016.

[22] T. Matsumoto, L.O. Chua, and K. Kobayashi, "Hyper chaos: laboratory experiment and numerical confirmation," *IEEE Transactions on Circuits and Systems*, vol. 33, no. 11, pp. 1143–1147, 1986.

[23] Y. Hong, M.W. Lee, and K.A. Shore, "Optimised message extraction in laser diode based optical chaos communications," *IEEE Journal of Quantum Electronics*, vol. 46, no. 2, pp. 253–257, 2009.

[24] O. Spitz, J. Wu, M. Carras, C.W. Wong, and F. Grillot, "Low-frequency fluctuations of a mid-infrared quantum cascade laser operating at cryogenic temperatures," *Laser Physics Letters*, vol. 15, no. 11, p. 116201, 2018.

[25] G.D. VanWiggeren and R. Roy, "Chaotic communication using time-delayed optical systems," *International Journal of Bifurcation and Chaos*, vol. 9, no. 11, pp. 2129–2156, 1999.

[26] K.M. Cuomo and A.V. Oppenheim, "Circuit implementation of synchronized chaos with applications to communications," *Physical Review Letters*, vol. 71, no. 1, p. 65, 1993.

[27] A. Sanchez-Diaz, C.R. Mirasso, P. Colet, and P. Garcia-Fernandez, "Encoded Gbit/s digital communications with synchronized chaotic semiconductor lasers," *IEEE Journal of Quantum Electronics*, vol. 35, no. 3, pp. 292–297, 1999.

[28] F. Grillot, O. Spitz, A. Herdt, W. Elsässer, and M. Carras, "Towards private optical communications with mid infrared chaotic light," *Proc. SPIE Photonics West*, Quantum Sensing and Nano Electronics and Photonics XVII, p. 112881P, February 2020.

[29] A. Bogris, A. Argyris, and D. Syvridis, "Encryption efficiency analysis of chaotic communication systems based on photonic integrated chaotic circuits," *IEEE Journal of Quantum Electronics*, vol. 46, no. 10, pp. 1421–1429, 2010.

[30] O. Spitz, J. Wu, A. Herdt, G. Maisons, M. Carras, W. Elsässer, C.W. Wong, and F. Grillot, "Extreme events in quantum cascade lasers," *Advanced Photonics*, vol. 2, no. 6, p. 066001, 2020.

[31] A. Uchida, *Optical communication with chaotic lasers: applications of nonlinear dynamics and synchronization*, John Wiley & Sons, 2012.

[32] O. Spitz, A. Herdt, J. Wu, G. Maisons, M. Carras, C.W. Wong, W. Elsässer, and F. Grillot, "Private communication with quantum cascade laser photonic chaos," *Nature Communications*, vol. 12, no. 1, pp. 1–8, 2021.

[33] T. Jüngling, X. Porte, N. Oliver, M.C. Soriano, and I. Fischer, "A unifying analysis of chaos synchronization and consistency in delay-coupled semiconductor lasers," *IEEE Journal of Selected Topics in Quantum Electronics*, vol. 25, no. 6, pp. 1–9, 2019.

[34] S. Breuer, W. Elsässer, J.G. McInerney, K. Yvind, J. Pozo, E.A.J.M. Bente, M. Yousefi, A. Villafranca, N. Vogiatzis, and J. Rorison, "Investigations of repetition rate stability of a mode-locked quantum dot semiconductor laser in an auxiliary optical fiber cavity," *IEEE Journal of Quantum Electronics*, vol. 46, no. 2, pp. 150–157, 2009.

[35] O. Spitz, A. Herdt, J. Duan, M. Carras, W. Elsässer, and F. Grillot, "Extensive study of the linewidth enhancement factor of a distributed feedback quantum cascade laser at ultra-low temperature," *Proc. SPIE Photonics West*, Quantum Sensing and Nano Electronics and Photonics XVI, p. 1092619, February 2019.